INTERNATIONAL ATOMIC ENERGY AGENCY
UNITED NATIONS EDUCATIONAL, SCIENTIFIC AND CULTURAL ORGANIZATION

INTERNATIONAL CENTRE FOR THEORETICAL PHYSICS
34100 TRIESTE (ITALY) - P.O.B. 586 - MIRAMARE - STRADA COSTIERA 11 - TELEPHONE: 2240-1
CABLE: CENTRATOM - TELEX 460392 - I

H4.SMR/285 - 11

WINTER COLLEGE ON
LASER PHYSICS: SEMICONDUCTOR LASERS
AND INTEGRATED OPTICS

(22 February - 11 March 1988)

QUANTUM WELLS FOR PHOTONICS

H. Melchior
Swiss Federal Institute of Technology
Zürich, Switzerland

[illegible]

New techniques for growing semiconductors with alternating ultrathin layers allow one to produce materials with made-to-order electro-optic properties and potential uses such as optical modulators and solid-state photomultipliers.

Daniel S. Chemla

PHYSICS TODAY / MAY 1985

The crystalline and electronic structures of semiconductors reflect a delicate balance of very large electromagnetic forces, and consequently minute compositional variations or small perturbations can induce large changes in the properties of these materials. For several decades now, research scientists and device designers have exploited this exceptional flexibility to tailor the electronic and optical properties of semiconductors for a variety of fundamental studies and applications. Semiconductor technology has made its most apparent impact, of course, in solid-state electronics.

In recent years, however, the field of photonics, which combines laser physics, electro-optics and nonlinear optics, has burgeoned. Modern lightwave communications exemplify photonic systems: Here optical signals are generated, modulated, transmitted and detected before they are transformed to electrical form for final use. Information processing is another example. Optical processing of information has several advantages over electronic processing, which must usually be done serially and is limited in speed by the broadening of pulses in interconnecting wires and is limited in density by "cross talk" between those wires. Optical systems capable of handling very large quantities of data await only the development of convenient digital optical logic elements with low switching energy.

Daniel Chemla is head of the quantum physics and electronics research department at AT&T Bell Laboratories, in Holmdel, New Jersey.

An ideal material for electro-optic applications such as those mentioned above would be able to transform light into current and vice versa for detection and emission. The material would also exhibit large electronic and optical nonlinearities that would allow one to use it as a transistor and optical gate. By taking advantage of both of these nonlinearities at the same time, one can use the material as an optical modulator. In the last decade we have seen the development of new methods for growing materials epitaxially. Techniques such as molecular beam expitaxy[1] and metal–organic chemical vapor deposition[2] combine an ultraclean growth environment and a slow growth rate to produce samples of extremely high quality. In particular, these techniques allow one to produce heterojunctions that are atomically abrupt and planar. With growth rates as low as 1 Å/sec, one can make layered structures with layer thicknesses ranging from a few angstroms to a few microns, as well as microstructures with continuously tuned composition profiles. These artificial media exhibit novel properties not shown by the parent compounds in the bulk.

Structures consisting of stacks of ultrathin layers are called superlattices or quantum-well structures,[3] and those with continuously varying compositions are called graded-gap structures. In this article I discuss the basic opto-electronic properties of quantum-well and graded-gap structures and describe some recent research that has potential applications in photonics.[4,5] I begin with a look at the physics of the layered structures, which feature band-gap discontinuities, or abrupt spatial changes in the energy gap between the valence band and the conduction band. Explaining the opto-electronic properties of these quantum-well structures will bring me to such topics as room-temperature excitons, optical nonlinearities and the behavior of carriers constrained to move in two dimensions only (figure 1). I will also say a few words about the structures whose compositions—and band-gap energies—vary smoothly. These graded-gap materials exhibit unusual energy-band gradients that imitate electric fields, which device designers can use to adjust the drift velocities of carriers over a large range. Finally, I will consider the wide variety of present and potential applications that discontinuous and graded-gap materials have in photonics. These applications range from mode-locking laser diodes and high-speed optical samplers to solid-state photomultipliers and optical gates with ultralow switching energies.

The materials. The compound III–V semiconductors, which are made from group-III and group-V elements, have the basic properties necessary for fabricating quantum-well and graded-gap materials. These semiconductors have a direct band gap, that is, they can emit or absorb light without the help of lattice vibrations, and thus they are very efficient absorbers and emitters. They also have large carrier mobilities and are easily doped. More importantly, they can form various solid solutions with identical crystal structures and well-matched lattice parameters but

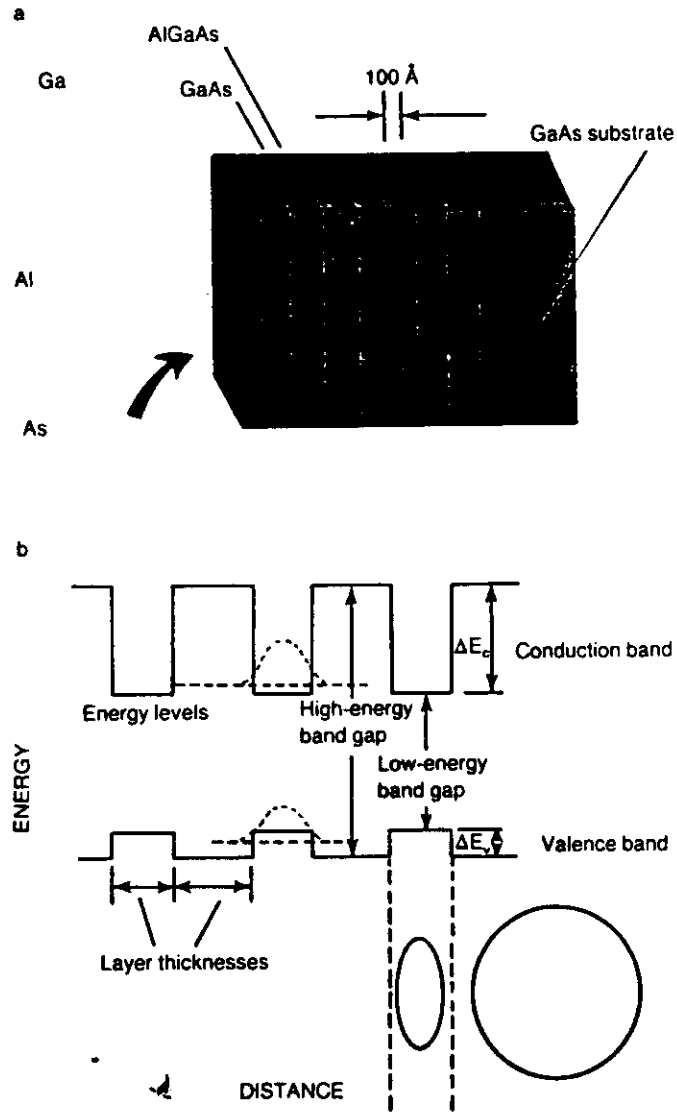

Quantum-well structure and corresponding real-space energy band structure. The schematic diagram in a shows compositional profiling in thin layers. The circle in b represents an exciton in the bulk compound, and the ellipse represents an exciton confined in a layer with a low band gap. Figure 2

with different energy gaps and refractive indices.

The chemical and physical compatibilities of solid solutions of various III–V compounds make it possible to grow heterostructures involving several compounds. One can make heterostructures with high-quality interfaces, and tailor the optical and electronic discontinuities for specific applications. Although structures have not yet been optimized for more than one function at a time, the III–V alloys could in principle be used for several functions at once. This possibility has motivated much of the tremendous effort over the last 20 years to synthesize III–V semiconductors, study and understand their fundamental characteristics and manipulate their properties. (See Venkatesh Narayanamurti's article on crystalline semiconductor heterostructures, PHYSICS TODAY, October, page 24.)

Physics and structure

Electrons and holes can propagate freely in the periodic potential of semiconductors. The major changes in the dynamics of these charged carriers caused by the semiconductor environment are: replacement of the free-electron masses by much smaller electron and hole effective masses, and a substantial increase in the dielectric constant. As a consequence of these changes, basic physical quantities such as the Bohr radius and the Rydberg constant are drastically modified in semiconductors. In the case of the III–V compounds, the Bohr radius ranges from 10 Å to 500 Å, corresponding to effective Rydberg constants ranging from 100 meV to 1 meV.

The change of scale in these natural units causes a number of processes involving electrons and holes in semiconductors to be different from the free-space atomic processes that they parallel. Thus carriers in semiconductors are more sensitive to small perturbations, a situation that one can exploit for device applications and that one can use to obtain model systems not encountered with free particles. In superlattices and graded-gap structures, modifications of free-particle behavior due to quantum size effects are important. Quantum size effects arise when the dimensions of a quantum system become comparable to the Bohr radius; one can observe these effects in semiconductor microstructures that have dimensions on the order of 100 Å.

The simplest examples of systems where size produces fundamental modifications of optical and electronic properties are quantum-well structures.[6] These structures consist of ultrathin layers of two or more compounds grown one on another periodically, as figure 2a indicates. Because the layers have different band gaps, the energy bands present discontinuities in real space, as shown schematically in figure 2b. Quantization of the carrier motion in the direction perpendicular to the layers produces a set of discrete energy levels. If the energy discontinuities are large enough and the layers with large band gaps are wide enough, then there will be little interaction between adjacent low-gap layers. The carriers confined in each of those layers will behave almost independently. Hence the name quantum-well structures. When the barriers are narrow, or when the energy of a state is comparable to the energy discontinuities, the interaction between layers is important. The wavefunctions of the carriers are extended perpendicularly to the layers, so the behavior of the carriers is modified by the periodic long-range modulation superimposed upon the crystalline potential. Hence the name superlattices.

In quantum-well structures, electrons and holes do not move with their usual three degrees of freedom. They show one-dimensional behavior normal to the layers and two-dimensional be-

Absorption spectrum of a GaAs–$Al_{0.3}Ga_{0.7}As$ quantum-well structure. The steps in this room-temperature spectrum mark transistions between sub-bands. The peaks at the edges of the steps are due to excitons. Figure 3

havior in the planes of the layers. This reduced dimensionality induces drastic changes in the electric and optical properties of quantum-well materials. For example, one can introduce impurities in the large-gap layers in such a way that the impurity nuclei will be trapped while the carriers that are introduced can migrate toward the low-gap layers and form two-dimensional gases at the interfaces. This technique, known as modulation doping,[7] produces a physical separation between impurities and carriers, leaving the carriers highly mobile. Solid-state physicists have taken advantage of the properties of two-dimensional electron gases in the fabrication of high-speed field-effect transistors and in fundamental studies on the integral and fractional quantum Hall effects.[8]

In layered structures, the conduction and valence bands become sets of two-dimensional sub-bands with step-like densities of states. This increases the number of states that contribute to the optical transitions at the absorption edge. Hence the absorption spectra of quantum-well structures are significantly different from those of three-dimensional semiconductors. Device designers have used this effect to obtain very-low-threshold diode lasers by including quantum wells in the active region of the diode.[9]

Excitons. For undoped quantum-well structures, excitonic effects are further modified by the confinement of carriers. As we will see later, optical effects associated with excitons play a crucial role in many opto-electronics applications of quantum-well structures. When a high-purity semiconductor absorbs a photon, the electron that is promoted to the conduction band interacts with the hole left in the valence band. The electron and hole can form a bound-state analog of the hydrogen atom called an exciton. This final-state interaction produces a set of discrete and very strong absorption lines just under the band gap. Because the binding energy of the exciton—the energy of its 1s state, or its effective Rydberg constant—is very small, excitons are very fragile. Excitons are sensitive to any kind of defect and are usually observed only at low temperature because they are easily broken apart by thermal phonons.

In a quantum-well structure with layer thicknesses smaller than the Bohr radius, the exciton has to modify its structure to fit into the low-gap layers. It flattens and shrinks. This is illustrated in figure 2b by the colored circle, which represents the 280-Å-diameter exciton of bulk GaAs, and by the ellipse, which represents the exciton when it is confined in a 100-Å quantum well. The electron and the hole are forced to orbit closer to each other, and the binding energy increases by a factor of two to three.

This added stability makes the exciton's resonances observable at room temperature, as demonstrated clearly by the absorption spectrum shown in figure 3. This spectrum was measured at room temperature in a high-quality quantum-well structure that Arthur Gossard grew at AT&T Bell Laboratories. The sample has 65 periods of 96-Å-thick layers of GaAs alternating with 98-Å-thick layers of $Al_{0.3}Ga_{0.7}As$. In figure 3 one can see the steps associated with the transitions between sub-bands, and one can see exciton peaks before each step. Exciton peaks as clearly resolved as this are usually seen only at very low temperature in bulk semiconductors of ultrahigh purity. The peaks are so apparent in quantum-well structures not only because of the increased exciton binding energy but also because the confinement strongly enhances the contrast with the continuum.[10] In bulk GaAs there is only one exciton resonance. The reduced symmetry of quantum-well structures, however, produces two valence bands and hence two excitons. This results in the double peak seen at the onset of the first transition. Similar exciton resonances, well resolved at high temperature, have been seen in the quantum-well material GaInAs–AlInAs, whose band gap is in the infrared.

It was at first thought that the room-temperature excitonic resonances in quantum-well structures simply offered a convenient way of making use of the large, intensity-dependent absorption and refraction effects usually seen at low temperatures in bulk semiconductors. Indeed quantum-well structures do have giant optical nonlinearities, but these originate from the novel physical properties of the layered structures and present a richer array of potential applications than do the nonlinearities observed at low temperatures in bulk crystals.

When light tuned to the exciton peak illuminates a quantum-well structure, bound electron–hole pairs are first generated and then quickly ionized by the large population of thermal phon-

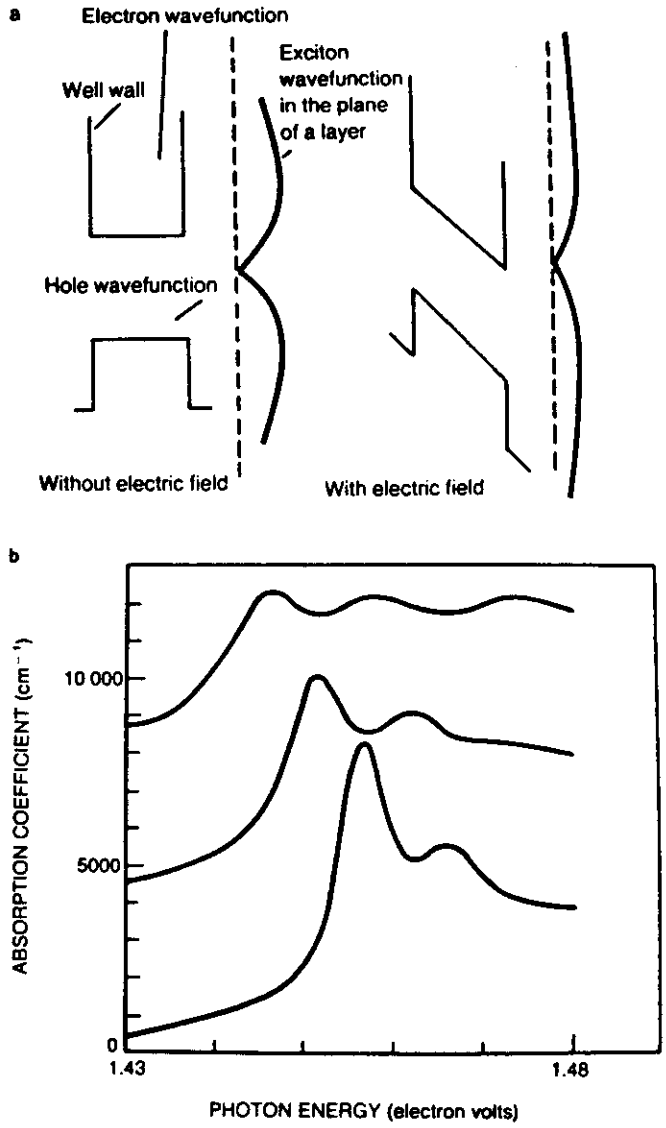

Excitonic wavefunctions without and with an applied electric field (a), and the quantum confined Stark shift in an absorption spectrum (b). The wavefunctions illustrate how the walls of a quantum well hold an electron and hole in a bound state, even at applied fields much stronger than the classical ionization field. The absorption spectra are those of a quantum-well structure under three different static electric fields applied normal to the layers. The fields are 10^4 V/cm (bottom curve), 5×10^4 V/cm (middle curve) and 7.5×10^4 V/cm (top curve). Figure 4

ons present at room temperature. At room temperature the average thermal energy kT is about three times larger than the exciton binding energy. Note for comparison that the ionization temperature for hydrogen atoms is about 2×10^5 K. Recent measurements with femtosecond optical spectroscopic techniques[11] found the ionization time of excitons in quantum-well structures to be 300 fsec. Due to the effects of the electron–hole plasma, the coefficient of absorption and the index of refraction depend strongly on the intensity of the incident light. These dependencies show up in measurements with continuous-wave laser light as well as with picosecond laser pulses. These nonlinearities are several orders of magnitude larger than those observed in normal semiconductors, yet they are still about half as large as the nonlinearities produced by the selective generation of excitons with femtosecond laser sources.[12]

It is commonly believed that the charged electron–hole plasma is more efficient than the neutral bound pairs in shielding electrostatic forces. This is true if the electrons and holes are at the same temperature. However, excitation with ultrashort optical pulses at the resonant frequency generates an exciton gas of temperature near 0 K that relaxes toward a warm electron–hole plasma of temperature around 300 K by absorbing phonons. This most unusual reversed relaxation, and the reduced strength of screening due to the reduced dimensionality in the quantum-well structure, together produce very large optical nonlinearities that have two stages—a stage lasting for subpicosecond times, corresponding to the time it takes for the exciton to ionize, and a stage lasting for nanoseconds, corresponding to the time it takes for the electron–hole pair to recombine.[10]

Excitons in quantum-well materials are also sensitive to electrostatic perturbations. Because the carrier wavefunctions extend to about 100 Å, and because the confinement or binding energies are only 10–100 meV, moderate electric fields of order 10 mV per 100 Å, or 10^4 V/cm, cause significant perturbations. When an electrostatic field is applied to a three-dimensional exciton, it induces a Stark effect analogous to that seen on atoms: There is a small shift in energy levels that is quickly masked because the energy levels are broadened by the exciton's ionization under the influence of the electric field. One sees this in quantum-well systems when the field is applied parallel to the planes of the layers.

With a perpendicular field, however, an absolutely new process occurs.[13] The field pushes the electron and the hole apart, but the wall of the well prevents ionization by constraining the particles to stay close enough to remain bound, as figure 4a indicates. The ionization can only occur when the particles tunnel out of the well. Consequently, it is possible to apply fields as large as 50 times the classical ionization field, inducing redshifts (figure 4b) in the absorption peak 2.5 times the binding energy, and still observe exciton resonances! This phenomenon, which figure 1 illustrates, is called the quantum confined Stark effect. Of course, one cannot create a similar situation for atoms, but quantum-well structures provide model systems in which one can study the effects of such extreme conditions and make tests against theory. The observed shifts due to the quantum confined Stark effect are well accounted for by the field-induced variations in the energy of the single-particle state and by pair attraction.[13] This effect also allows one to shift an abrupt and highly absorbing edge into a spectral region where the sample is normally transparent. Such shifts have obvious applications in optical modulation and optical logic, and I will discuss these below.

As figure 2b indicates, the conduction band and the valence band do not contribute equally to the total bandgap discontinuity at a heterojunction. Recent measurements[14] on a GaAs–AlGaAs quantum-well structure, for

High-speed optical modulator and its optical response to an electrical pulse. The schematic diagram shows a p–i–n diode with a quantum-well optical modulator. The speed of the device is limited by the circuit's RC constant and by the large diameter of the quantum-well structure. Figure 5

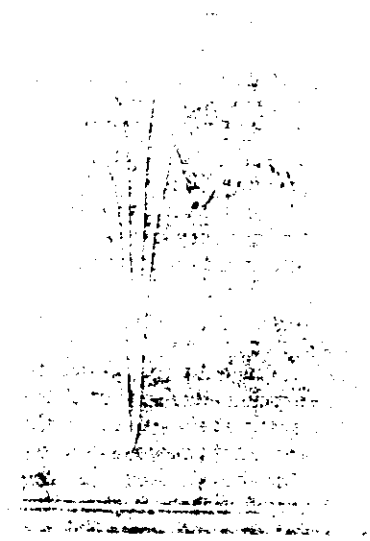

example, indicate that ΔE_c, the change in the energy level of the bottom of the conduction band as one crosses a heterojunction, is about -1.5 times ΔE_v, the change in the energy level of the top of the valence band across the junction. This intrinsic asymmetry between electrons and holes can produce spectacular effects such as impact ionization, which depends critically on energy gains at heterojunctions. As we will see, new types of photodetectors take advantage of this asymmetry.

Graded gaps. So far we have discussed only discontinuous heterojunctions. There is, however, a more subtle way to engineer band structure: by playing with the composition profile. A continuous spatial variation of the composition induces a gradient of the energy bands equivalent to an internal electric field, and because the valence and conduction bands experience different discontinuities, the effective fields seen by holes and electrons are not the same.[5] One can use this new degree of freedom to produce complex internal field profiles, and thus to act locally on the carrier drift velocity. For example, experimenters have measured[15] an equivalent field of order of 10^4 V/cm in a linearly graded gap structure made from $Al_xGa_{1-x}As$. Such a field can accelerate electrons to velocities as high as 2×10^7 cm/sec.

Microstructures for photonics

The special properties of quantum-well materials suit them to a variety of applications in photonics. Below I consider some of these properties and applications.

The optical nonlinearities of quantum-well structures close to the band edge are the largest measured so far in any semiconductor at room temperature. Because quantum-well structures are easily tuned to laser-diode wavelengths, they have been used in applications where one wants a small amount of excitation to produce a large change in absorption or refraction.

Short-pulse light sources. Passive mode locking of laser diodes allows for compact and efficient short-pulse light sources. However, the design of such mode-locking diodes has suffered from a shortage of adequate saturable absorbers with large enough cross section and short recovery time. Recent experiments on quantum-well structures implanted with light ions have shortened to 150 psec the recombination time of carriers generated by the ionization of excitons. Solid-state physicists have used these fast-recovery saturable absorbers to make stable and reliable mode-locking laser diodes. Such diodes, made from GaAs, have emitted[16] pulses as short as 1.6 psec, the shortest regular pulse trains yet delivered by a diode laser.

Optical switches in cavities. Experiments have demonstrated[17] optical bistability in a sample of quantum-well material held in a Fabry–Perot resonator. Theory indicates[18] that optical switches made from quantum-well materials in precisely tuned etalons will have very low switching energies

High-speed optical modulators. Recent experiments have used the quantum confined Stark effect to achieve the high-speed modulation of light from laser diodes. To build such a modulator, one grows a quantum-well structure in the intrinsic region of a p–i–n diode, as figure 5 shows. By putting a reverse bias on the resulting device, one applies a field without causing current to flow. When the modulator represented in figure 5 was given a 122-psec electrical pulse, it subjected the laser light passing through it to a 131-psec 2.3-dB attenuation. The modulator's response was limited by the effects of capacitance in its 95-micron-diameter structure.[19] The speed of the quantum confined Stark effect is limited only by how quickly the exciton envelope function can follow the applied field. At present, however, the limit is how fast one can change the applied field, so faster operation should be feasible with devices having smaller areas and therefore smaller capacitances. The quantum-well structure that imposed the 2.3-dB modulation

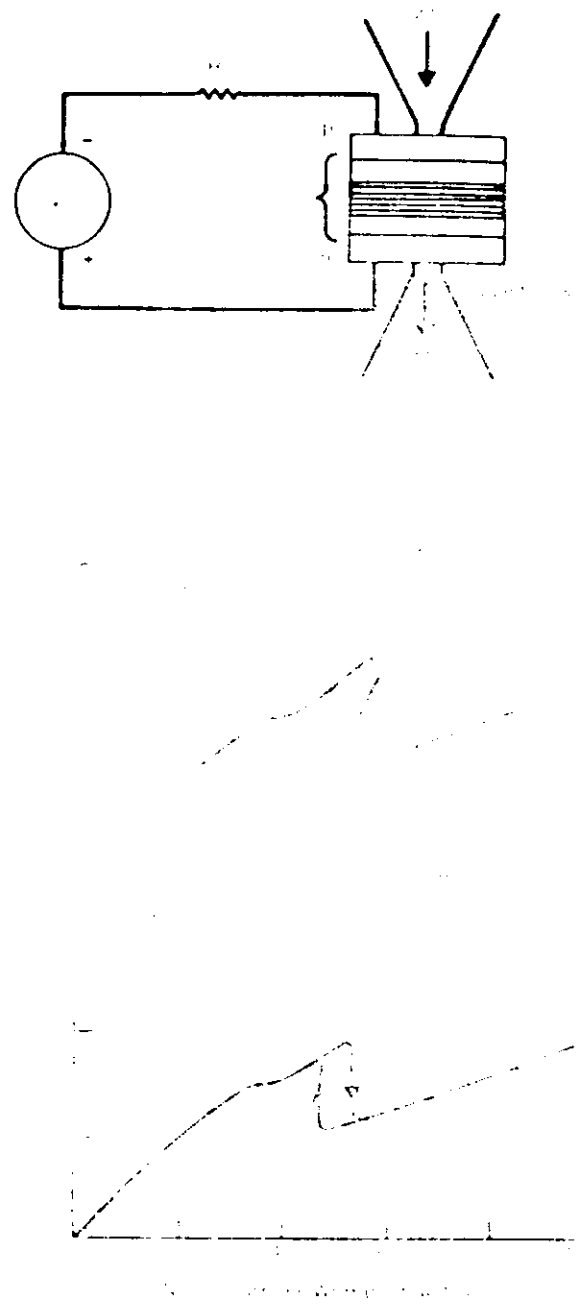

Self-electro-optic device and plots showing its optical bistability. The device in the schematic diagram shows optical bistability when it is connected to a simple resistive load. Figure 6

was only about one micron thick; longer light paths increase the attenuation considerably.

Self-electro-optic devices. When a photon is absorbed in a quantum confined Stark effect p–i–n structure, it generates an electron–hole pair that is separated by the field; here the modulator behaves like a photodetector of unit quantum efficiency. The ability of such a p–i–n device to act as both a modulator and a photodetector provides an internal feedback mechanism when the device is connected to an electronic circuit. This is the basis of a new category of devices, known as self-electro-optic devices, that can operate as optical gates with very low switching energy, self-linearized modulators and optical level shifters.[20]

The optical gate represented in figure 6a operates as follows: One applies just enough voltage to the device to shift the absorption edge so that there is little absorption at the exciton peak; then one directs a light beam of varying intensity onto the device. As the beam's intensity increases, it generates a photocurrent that induces a voltage drop across the resistor. The voltage across the device decreases, the edge shifts back and the absorption increases, increasing the photocurrent. This cycle continues until the device switches to a state of low transmission. The switch back to a highly transmitting state does not occur at the same incident intensity because the self-electro-optic device is now absorbing. Therefore the gate response, shown in figure 6b, is an optical hysteresis loop.

The self-electro-optic devices demonstrated to date typically have total switching energies of 20 fJ per square micron. This switching energy is only one-sixth that reported for any other optically bistable device, despite the fact that self-electro-optic devices operate without resonant cavities. The total switching energy comprises two parts: resonant optical energy, which accounts for about 20% of the total, and electrical energy, which accounts for the other 80%. Self-electro-optic devices are compatible with other III–V semiconductor technologies, and should fit into large-scale integrated arrays.

High-gain avalanche photodetectors can be built from a solid with a large difference between the rates at which electrons and holes create electron–hole pairs throughout impact ionization. In gallium arsenide, unfortunately, the two ionization rates are about the same. Furthermore, avalanche multiplication is intrinsically a noisy process because of the randomness of the ionization events, and that causes statistical fluctuations in the gain. New concepts based on quantum-well and graded-gap structures have overcome these obstacles. Figure 7a shows the band structure of a p–i–n diode that contains a quantum-well structure in its intrinsic region. When a hot electron enters a gallium arsenide quantum well, it suddenly gains an energy ΔE_c. The ionization threshold for electrons is thus reduced from ΔE_{th} to $\Delta E_{th} - \Delta E_c$, whereas for the holes it is reduced to $\Delta E_{th} - \Delta E_v$. Because the ionization rates depend exponentially on the thresholds, one can greatly enhance the ratio of electron and hole ionization rates. AlGaAs–GaAs avalanche photodetectors have shown[21] ratios as large as seven. The performances can be improved further by using a sawtooth profile with regions of linear grading followed by abrupt steps, as shown in figure 7b. When one applies a static field to the structure, figure 7c, the impact ionization events occur at each step deterministically, and preferentially for the electrons. The resulting multiplication processes are no longer random, and the gain is almost noise free. The graded-gap structure acts as a solid-state photomultiplier, with the steps in the energy bands corresponding to the dynodes of a traditional photomultiplier tube.[21]

Fast transistors. The transit time of

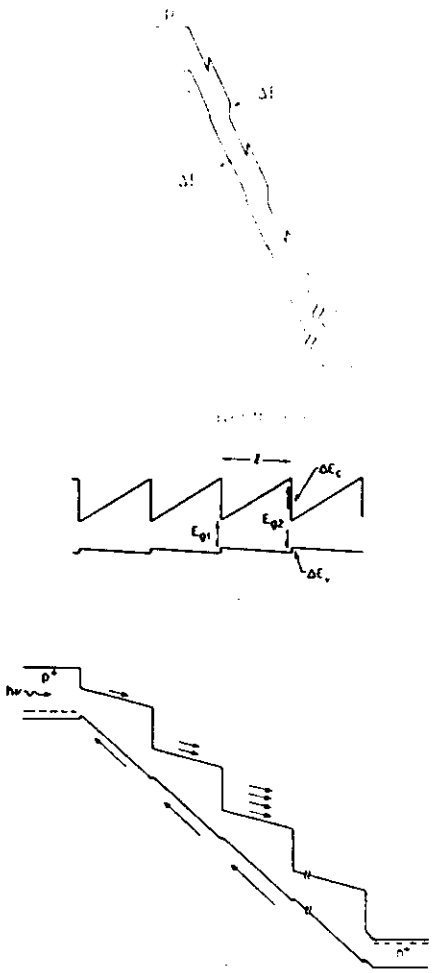

Band structures. a: Band structure of an avalanche photodetector made from a p–i–n quantum-well structure. b: Band structure of a sawtooth graded-gap multilayer structure. The composition varies linearly from the low-gap compound to the large-gap compound and then abruptly switches back to the low-gap composition. c: Band structure of a graded-gap solid-state photomultiplier with an applied bias voltage. The arrows illustrate how the electrons multiply by impact ionization at discontinuities in the conduction band whereas the holes do not gain enough energy at valence-band discontinuities to participate in impact ionization. Figure 7

the minority carriers in the base of a transistor is governed by diffusion. Almost three decades ago, H. Kroemer of RCA proposed[22] introducing quasielectric fields in the base of a transistor to reduce the carrier transit time. Experimenters recently succeeded in doing this in a phototransistor with a wide-band-gap emitter and a graded-gap base. The 10^4 V/cm quasifield in the base gave an intrinsic response time of 20 psec—less than one-fifth of the diffusion time of carriers in an identical structure without a graded base.[21] Further improvements under study include the ballistic launching of electrons into the base by a conduction-band discontinuity at the emitter–base heterojunction.

The examples I have given of semiconductor properties that are strongly modified by quantum size effects and compositional profiling are just a limited set chosen for their relevance to photonics. In principle, we can use abrupt heterojunctions, selective doping and continuous composition grading to engineer, in almost any arbitrary fashion, the energy-band structure of semiconductor microstructures. The recently developed epitaxial growth techniques already allow us to control the compositions of samples along one dimension. We can envision new techniques that in the near future will give us atomic-scale control over growth in three dimensions. This will enable us to tailor the local band structure of samples according to specific designs. There is no doubt that the resulting materials will present new properties—some unsuspected—and that these new properties will give rise to new applications.

References

1. See, for example, L. L. Chang, K. Ploog, eds., *Molecular Beam Epitaxy and Heterostructures*, NATO Advanced Science Institute Series, Nijhoff, Dordrecht (1985).
2. See, for example, J. B. Mullin, S. J. C. Irvine, R. H. Moss, P. N. Robson, D. R. Wight, eds., *Metal Organic Vapor Phase Epitaxy 1984*, North-Holland, Amsterdam (1984).
3. L. Esaki, R. Tsu, IBM J. Res. Dev. **14**, 61 (1970); for an outline of the history of Esaki's and Tsu's discovery, with Leroy Chang, of artificial semiconductor superlattices, PHYSICS TODAY, March, p. 87.
4. See, for example, D. S. Chemla, D. A. B. Miller, P. W. Smith, *Device and Circuit Applications of III–V Semiconductor Superlattices and Modulation Doping*, R. Dingle, ed., Academic, New York (1985).
5. See, for example, F. Capasso, *Device and Circuit Applications of III–V Semiconductor Superlattices and Modulation Doping*, R. Dingle, ed., Academic, New York (1985).
6. R. Dingle, *Festkörperprobleme* **15**, H. J. Queisser, ed., Pergamon, Braunschweig (1975).
7. R. Dingle, H. L. Stormer, A. C. Gossard, W. Wiegmann, Appl. Phys. Lett. **33**, 665 (1978); H. L. Stormer, Surf. Sci. **132**, 519 (1983).
8. T. Mimura, S. Hiyamizu, T. Fujii, K. Nambu, Japan J. App. Phys. **19**, L225 (1980); D. Delagebeaubeuf, P. Delescluse, P. Etienne, M. Laviron, J. Chaplart, N. T. Linh, Electron Lett. **16**, 667 (1980); H. L. Stormer, *Festkörperprobleme* **24**, P. Grosse, ed., Vieweg, Braunschweig (1984).
9. See Y. Suematsu's article on page 32 of this issue.
10. D. S. Chemla, D. A. B. Miller, J. Opt. Soc. Am. B, to be published July 1985.
11. C. V. Shank, Science **219**, 1031 (1983).
12. W. H. Knox, R. F. Fork, M. C. Downer, D. A. B. Miller, D. S. Chemla, C. V. Shank, Proc. Fourth Int. Conf. Ultrafast Phenomena, Springer-Verlag, Berlin (1984), p. 162; Phys. Rev. Lett. **54**, 1306 (1985).
13. D. A. B. Miller, D. S. Chemla, T. C. Damen, A. C. Gossard, W. Wiegman, T. H. Wood, C. A. Burrus, Phys. Rev. Lett. **53**, 2173 (1984).
14. R. C. Miller, A. C. Gossard, D. A. Kleinman, O. Munteanu, Phys. Rev. B**29**, 3740 (1984); for a review of exciton spectroscopy in quantum-well structures, see R. C. Miller, D. A. Kleinman, Proc. 3rd Trieste IUPAP Semiconductor Symp., J. Lumin. **30**, 520 (1985).
15. B. F. Levine, C. G. Bethea, W. T. Tsand, F. Capasso, K. K. Thornber, R. C. Fluton, D. A. Kleinman, Appl. Phys. Lett. **43**, 769 (1983).
16. Y. Silberberg, P. W. Smith, D. J. Eilenberger, D. A. B. Miller, A. C. Gossard, W. Wiegmann, Optics Lett. **9**, 507 (1984).
17. H. M. Gibbs, S. S. Tarng, J. L. Jewell, D. A. Weinberger, K. Tai, A. C. Gossard, S. L. McCall, A. Pasner, W. Wiegmann, Appl. Phys. Lett. **41**, 221 (1982).
18. P. W. Smith, Proc. Conf. Electro '83, session record 11/1, IEEE, New York (1983).
19. T. H. Wood, C. A. Burrus, D. A. B. Miller, D. S. Chemla, T. C. Damen, A. C. Gossard, W. Wiegmann, IEEE J. Quantum Electron. **QE-21**, 117 (1985).
20. D. A. B. Miller, D. S. Chemla, T. C. Damen, A. C. Gossard, W. Wiegman, T. H. Wood, C. A. Burrus, Appl. Phys. Lett. **45**, 13 (1984); Optics Lett. **9**, 567 (1984); to be published in IEEE J. Quantum Electron. (1985).
21. F. Capasso, Sur. Sci. **513**, 142 (1984).
22. H. Kroemer, RCA Rev. **18**, 332 (1957). □

8 LIN, CHINLON, EISENSTEIN, G., TUCKER, R. S., BESOMI, P., and NELSON, R. J.: '11·2 GHz picosecond optical pulse generation in gain-guided short cavity InGaAsP injection lasers by high frequency direct modulation', *Electron. Lett.*, 1984, **20**, pp. 238–240
9 SU, C. B., and LANZISERA, V.: 'Effect of doping level on the gain constant and modulation bandwidth of InGaAsP semiconductor lasers', *Appl. Phys. Lett.*, 1984, **45**, pp. 1302–1304
10 LIAU, Z. L., and WALPOLE, J. N.: 'Novel techniques for GaInAsP/InP buried heterostructure laser fabrication', *ibid.*, 1982, **40**, pp. 568–570
11 SCHLAFER, J., SU, C. B., ROWAZINIK, W., and LAUER, R. B.: '20 GHz bandwidth InGaAs photodetector for microwave optical transmission', (to be published)

ELECTRIC-FIELD-INDUCED REFRACTIVE INDEX VARIATION IN QUANTUM-WELL STRUCTURE

Indexing terms: Semiconductor devices and materials, Quantum-well structures

The refractive index variation in a quantum-well structure by an electric field is given theoretically. The calculated variation is -1% for an applied field of $3{\cdot}1 \times 10^5$ V/cm in a 300 Å-thick GaInAsP/InP single quantum well, which is about 39 times larger than the bulk value. A semiconductor quantum-well structure is found theoretically to be a new material with a larger electro-optic coefficient. Application to a new optical switching device is also suggested.

Introduction: Electro-optic materials are widely used in the optoelectronics field. However, the refractive index variation Δn, n due to the electro-optic coefficient is relatively small in materials commonly used until now: the order of magnitude of Δn n is about 0·1% for $LiNbO_3$ crystal in conventional use, and 0·01% for III-V semiconductor bulk crystals. Although $\Delta n/n$ as large as 1% is obtained using the effect of carrier injection into semiconductors,[1] the response time of this effect is not rapid, limited by the carrier recombination time of a few nanoseconds.

The absorption loss variation in the quantum wells (QWs) due to an electric field has been reported recently.[2] However, the refractive index variation in a QW due to an electric field application has not yet been reported.

In this letter, we give a theoretical estimation of the refractive index variation due to an electric field applied perpendicular to the QW layers. It is shown that the magnitude of the refractive index variation is very much larger than that of commonly used bulk crystals with potential high-speed response.

Electric-field-induced refractive index variation: By an electric field applied perpendicular to the QW layers, the square-well potential in a QW is inclined. This change brings about the change in absorption spectra by the following two effects: (i) the change in energy eigenvalues in the QW, and (ii) separative polarisation of the wave functions of electrons and holes. Owing to (ii), couplings of electrons and holes between the same quantisation numbers of energy levels are reduced, and couplings between different quantisation numbers occur.

Because the absorption is related to the refractive index by the Kramers–Kronig relationship, the refractive index also changes due to the effects (i) and (ii) mentioned above.

We calculated the refractive index variation according to this qualitative discussion. The excitonic effect is not included in the present analysis. The wave functions of electrons in a single quantum well (SQW) polarised by electric field application were expanded with the wave functions without the field, and expansion coefficients were calculated by the secular equation resulting from the Schroedinger equation. Diagonalising the matrix composed of the coefficients of the secular equation, we obtained the energy levels and expansion coefficients of the wave functions. Using this result, we calculated the dipole moment for optical transition as in Reference 3, as a function of applied field E_0. Using this dipole moment and energy levels, the refractive index determined by electron-hole pairs is given by density matrix theory[3,4] as

$$n_d(E_0) = m_c^* m_v^*/(m_c^* + m_v^*)/(2n\varepsilon_0 \pi h^2 a) \times \sum_{l,m} \int_{E_{el}(E_0)+E_{vm}(E_0)+E_g}^{\infty} \langle R_{ch}^2(E_0)\rangle_{lm} \times \frac{(f_c - f_v)(h\omega - E_{ch})}{(h\omega - E_{ch})^2 + (h/\tau_{in})^2}\, dE_{ch}$$

where n is the index of a QW structure without electron-hole pairs, a is the well width, $\langle R_{ch}^2(E_0)\rangle_{lm}$ is the mean square of the dipole moment formed by an electron in sub-band l and a hole in sub-band m, and τ_{in} is the intraband relaxation time. The refractive index variation Δn is given by $n_d(E_0) - n_d(0)$. Because the interaction of the dipole moment with the TE-mode electromagnetic waves is much larger than that with TM-modes,[3] only TE-mode waves were assumed here. The light-hole band was neglected because of its small effective mass. Also neglected was the leakage of electrons tunnelling through the triangular potential barrier under the field application, assuming thick barrier width. Details of the calculations will be reported elsewhere.

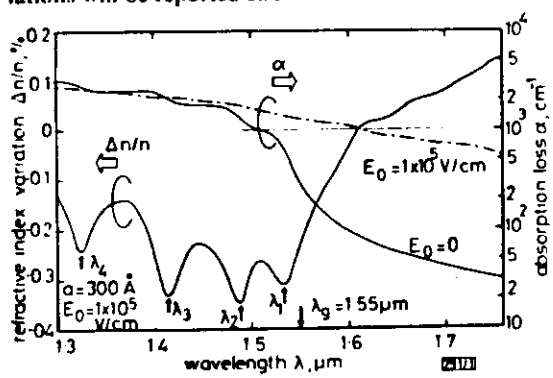

Fig. 1 *Spectra of refractive index variation and absorption loss for a 300 Å-thick GaInAsP/InP quantum well applied with electric field of 1×10^5 V/cm*

λ_1, λ_2 ... are wavelengths between the same quantised energy levels

Fig. 1 shows the spectral dependence of the refractive index variation and the absorption due to the electric field of 1×10^5 V/cm in a $Ga_{0.42}In_{0.58}As_{0.9}P_{0.1}$/InP 300 Å-thick SQW, the bulk bandgap of which is 0·8 eV (1·55 μm in wavelength). As seen in Fig. 1, the refractive index variation is negative in the wavelength region shorter than the bandgap and positive in the region longer than the bandgap. Peaks corresponding to the quantised energy levels (λ_1, λ_2 ...) are seen.

Fig. 2 shows the applied field dependence of the refractive index variation at different wavelengths. As can be seen, the variation increases negatively approximately in proportion to the applied field. $\Delta n/n = (n^2 r_{\perp,TE}/2)E_0$ (linear approximation), where $r_{\perp,TE}$ is the mean value of the equivalent electro-optic coefficient of the QW structure for polarisation parallel to the well, obtained as -1% at the field of $3{\cdot}1 \times 10^5$ V/cm at $\lambda = 1{\cdot}534$ μm ($= \lambda_1$). The ratio of $\Delta n/n$ to E_0, $n^2 r_{\perp,TE}/2$, is

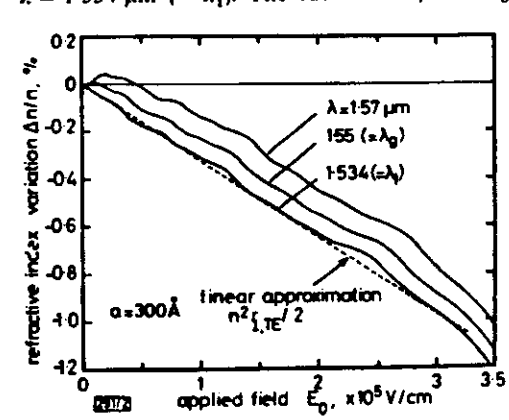

Fig. 2 *Refractive index variation as a function of applied field*

and $n^2 r_{41}/2$ to be about 7.7×10^{-9} cm/V and 7.8×10^{-10} cm/V, respectively,[5,6] and the former is 1/4 and the latter is 1/39 times that of the QW structure mentioned above. Thus the QW is found theoretically to be a new material with a large electro-optic coefficient. Also, the QW is an electro-optic material with an anisotropic property for light polarisation dominating in the TE-mode.[3]

One of the applications of a large refractive index variation in a QW structure is an optical switch using total internal reflection with two waveguides crossing each other. The angle between the two waveguides in this switch is about 11·5° at $E_0 = 3.1 \times 10^5$ V/cm, assuming the optical confinement factor of the waveguides to be 0·5, which shows a capability of small-size fabrication. High-speed operation is also expected as in the modulators.[2,7] Although the absorption loss coefficient is large as seen in Fig. 1, this absorption loss does not affect the properties in this total-internal-reflection-type switch because of the short path of the light through the QW waveguide.

Conclusion: We have analysed the refractive index variation due to an electric field applied to the QW. The index variation was obtained to be -1% for an applied field of 3.1×10^5 V/cm in a 300 Å-thick GaInAsP/InP SQW, which is much larger than the bulk values, and the QW is found theoretically to be a new electro-optic material with a large electro-optic coefficient. A possible new optical switching device using this effect is expected to be of small size and high speed.

Acknowledgments: The authors would like to thank Prof. K. Iga, Assoc. Prof. K. Furuya, Assoc. Prof. M. Yamada and Dr. H. Yamamoto for their helpful discussions. This work was supported by a scientific grant-in-aid from the Ministry of Education, Science & Culture of Japan.

H. YAMAMOTO
M. ASADA
Y. SUEMATSU

Department of Physical Electronics
Tokyo Institute of Technology
2-12-1 O-okayama, Meguro-ku, Tokyo 152, Japan

30th April 1985

References

1 TOHMORI, Y., SUEMATSU, Y., TSUSHIMA, H., and ARAI, S.: 'Wavelength tuning of GaInAsP/InP integrated laser with butt-jointed built-in distributed Bragg reflector', *Electron. Lett.*, 1983, **19**, pp. 656–657
2 WOOD, T. H., BURRUS, C. A., MILLER, D. A. B., CHEMLA, D. S., DAMEN, T. C., GOSSARD, A. C., and WIEGMANN, W.: 'High-speed optical modulation with GaAs/GaAlAs quantum wells in a p-i-n diode structure', *Appl. Phys. Lett.*, 1984, **44**, pp. 16–18
3 ASADA, M., KAMEYAMA, A., and SUEMATSU, Y.: 'Gain and intervalence band absorption in quantum-well lasers', *IEEE J. Quantum Electron.*, 1984, QE-20, pp. 745–753
4 YAMADA, M., and SUEMATSU, Y.: 'Analysis of gain suppression in undoped injection lasers', *J. Appl. Phys.*, 1981, **52**, pp. 2653–2664
5 KAMINOW, I. P., and TURNER, E. H.: 'Linear electrooptical materials', *in* PRESSLEY, R. J. (Ed.): 'Handbook of lasers with selected data on optical technology' (The Chemical Rubber Co., Cleveland, USA, 1971), p. 452
6 TADA, K., and SUZUKI, N.: 'Linear electrooptic properties of InP', *Jpn. J. Appl. Phys.*, 1980, **19**, pp. 2295–2296
7 YAMANISHI, M., and SUEMUNE, I.: 'Quantum mechanical size effect modulation light sources—A new field effect semiconductor laser or light emitting device', *ibid.*, 1983, **22**, pp. L22–L24

p-CHANNEL GaAs SIS (SEMICONDUCTOR-INSULATOR-SEMICONDUCTOR) FET

Indexing terms: Semiconductor devices and materials, Field-effect transistors, Semiconductor-insulator-semiconductor devices

The first *p*-channel GaAs SIS (semiconductor-insulator-semiconductor) FET having a p^+-GaAs/undoped GaAlAs/undoped GaAs structure is reported. The FET fabricated shows a transconductance of $g_m = 30$ mS/mm, a drain conductance of $g_d = 2.5$ mS/mm and a threshold voltage of $V_{th} = +0.2$ V at 77 K in the dark.

Recently we reported an *n*-channel GaAs SIS (semiconductor-insulator-semiconductor) FET in which an n^+-GaAs layer is used as a gate, an undoped GaAlAs layer as an insulator and an undoped GaAs layer as a semiconductor, and it has a self-aligned source and drain structure.[1] The GaAs SISFET inherits most of the best features of a MODFET. The FET also features a uniform threshold voltage because the GaAlAs layer is undoped, by the small variation of the threshold voltage with the variation of the temperature[2] because the GaAlAs layer is free of the DX centre, and by the simple fabrication process. On the other hand, it has been shown that by adopting the modulation-doped heterostructure the hole mobility can be enhanced to be $\sim 4 \times 10^4$ cm^2/V s with a hole concentration of $\sim 3.8 \times 10^{11}$/cm^2 at around 10 K.[3] A *p*-channel GaAs MODFET has been shown to have a transconductance of ~ 30 mS/mm.[4] We expect that a *p*-channel GaAs SISFET has the same advantages over the *p*-channel MODFET as the *n*-channel SISFET has over the *n*-channel MODFET, so the SISFET is attractive for GaAs complementary logic.

In this letter we report the first *p*-channel GaAs SISFET, in which a p^+-GaAs layer is used as a gate, an undoped GaAlAs layer as an insulator and an undoped GaAs layer as a semiconductor, and it has self-aligned source and drain p^+-layers.

The structure of the fabricated SISFET is shown in Fig. 1. A crystal of the following structure was grown by MBE: SI LEC (100)-GaAs substrate/undoped GaAs (1·5 μm)/undoped $Ga_{0.5}Al_{0.5}As$ (0·05 μm)/p^+-GaAs (Be-doped, 1×10^{18} cm^{-3}, 0·5 μm). The top p^+-GaAs layer was selectively etched off leaving a strip of 2 μm in length and 40 μm in width which worked as the gate. Using the p^+-GaAs gate as a mask, 1.5×10^{14} cm^{-2} Mg ions were implanted at 150 keV for the source and drain p^+-layers. The p^+-GaAs gate is so thick that it can sufficiently protect the invasion of the Mg ions into the GaAlAs layer. The sample was then annealed in an infra-red lamp furnace at 800 C for 30 s without a cap, under arsenic pressure. After selectively etching the GaAlAs layer, source and drain ohmic contacts, 8 μm apart, were formed with Cr/Au by alloying at 440°C for 1 min.

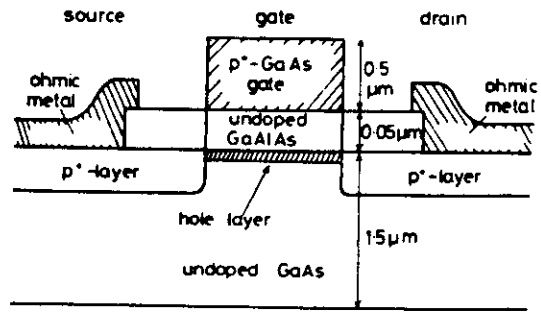

Fig. 1 *Schematic structure of p-channel GaAs SISFET*
Gate length is $L_g = 2$ μm; gate width $W_g = 40$ μm

The gate-source diode characteristic of a typical GaAs SISFET with the drain terminal open at 77 K in the dark is shown in Fig. 2. The forward current at the applied gate bias of $V_g = -1$ V is 40 μA and the reverse current at $V_g = +2.5$ V is also 40 μA. Thus the GaAlAs layer acts as a barrier layer for holes, and the diode shows a good rectifying behaviour.

The source current I_s against the drain-source voltage V_{ds} characteristics of the GaAs SISFET measured at 77 K in the dark is shown in Fig. 3. The gate bias is applied from $V_g = +0.4$ V to -1 V. The current increases along the square law with the V_g step. The threshold voltage at which the current reaches 40 μA is $V_{th} = 0.2$ V at $V_{ds} = -1$ V. The trans-